Supplemental Material to the article

"Magnetic Properties of Topological Kondo Insulator SmB_6: Localized Magnetic Moments and Pauli Paramagnetism"

The problem of finding of the localized magnetic moments (LMM) contribution, which appears in SmB_6 for $T < T^*$, is reduced to subtraction of Pauli contribution from the total magnetization

$$M_{\rm LMM}(B,T) = M(B,T) - M_{\rm Pauli}(B,T), \tag{S1}$$

where $M_{\rm Pauli}(B,T)$ contains both linear and non-linear parts. When the correction for the density of states $\Delta\rho(B,T)$ caused by renormalization is accounted apart constant value $\chi_1 = \chi_{10}$ in Eq. (2), Pauli magnetic susceptibility acquires the form $\chi_1(B,T) = \chi_{10} + \Delta\rho(B,T)\mu_{\rm B}^2$ and the derivative of the magnetic moment will be given by

$$\partial M_{\rm LMM}/\partial B = \partial M/\partial B - \partial M_{\rm Pauli}/\partial B = \partial M/\partial B - (\chi_{10} + \Delta\rho_0(B,t)\cdot(1 + \partial \ln \Delta\rho_0/\partial \ln B)\mu_{\rm B}^2). \tag{S2}$$

Here parameter χ_{10} describes linear part of Pauli magnetization and the term $\Delta\rho_0(B,T)\cdot(1 + \partial \ln \Delta\rho_0/\partial \ln B)\mu_B^2$ describes non-linear part. The "baseline" $\partial M_{\rm Pauli}/\partial B$ can be found from experiment for $T > T^*$ (region II in Fig. 2b of the main text), where $B_0(T) = {\rm const}$ and contribution of LMM is missing. In the diapason $T < T^*$, the function $\partial M_{\rm Pauli}/\partial B$ may be obtained by extrapolation. As long as χ_{10} does not depend on temperature and non-linear part of $\partial M_{\rm Pauli}/\partial B$ may be well described by equation $M_{s\rm Pauli}(T)/B_0 \cosh^2(B/B_0)$, it is sufficient to set dependence $M_{s\rm Pauli}(T)$ in the diapason $T < T^*$ and use temperature independent values of χ_{10} and B_0 corresponding to the range $T > T^*$. The linear extrapolation and second order polynomial extrapolation for the $M_{s\rm Pauli}(T)$ function were probed (curves *1* and *2* in Fig. 2b of the main text). Finding of the LMM contribution in accordance with the described procedure is illustrated by Fig. 1S. After subtraction from initial $\partial M/\partial B$ dependence (Fig. 1S, a, curve *1*) of the extrapolated curve $\partial M_{\rm Pauli}/\partial B$ (Fig. 1S, a, curve *2*), the derivative $\partial M_{\rm LMM}/\partial B$ may be obtained (Fig. 1S, b).

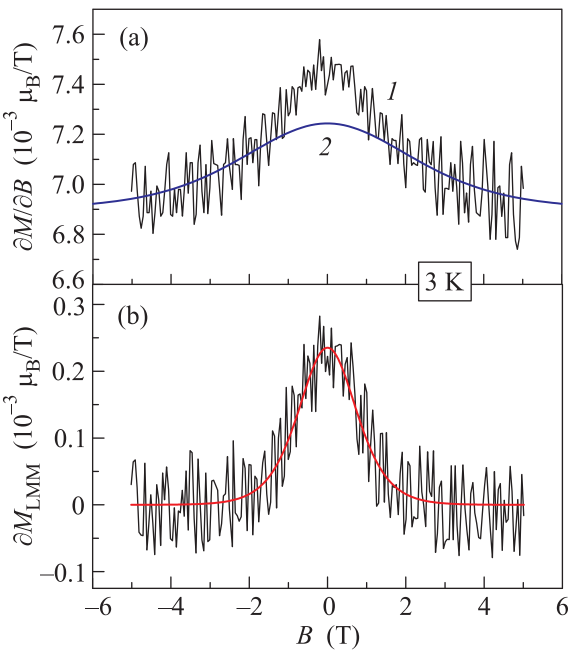

Fig. 1S. Subtraction of the localized magnetic moments contribution taking field dependence $\partial M/\partial B$ for $T = 3$ K as an example. (a) – *1* – initial $\partial M/\partial B$ data, *2* – $\partial M_{\rm Pauli}/\partial B$ approximation. (b) – Demonstrate difference curve $\partial M_{\rm LMM}/\partial B = \partial M/\partial B - \partial M_{\rm Pauli}/\partial B$ and its approximation with the help of Eq. (S3)

After that, the field dependence $\partial M_{\rm LMM}/\partial B$ was described by equation

$$\frac{\partial M_{\rm LMM}}{\partial B}=\frac{M_{s\rm LMM}}{B_{0\rm LMM}}\left(\left[\frac{1}{2J\sinh(B/2J\cdot B_{0\rm LMM})}\right]^2-\left[\frac{(1+1/2J)}{\sinh((1+1/2J)B/B_{0\rm LMM})}\right]^2\right), \tag{S3}$$

which corresponds to Brillouin function with a quantum number J. If the J value is fixed, the problem is reduced to two-parameter fitting with $M_{s\rm LMM}$ and $B_{0\rm LMM}$ (an example for the case $J=1/2$ is shown in Fig. 1S, b by smooth line).

In order to find temperature dependences $M_{s\rm LMM}(T)$ and $B_{0\rm LMM}(T)$, the data $\partial M_{\rm LMM}/\partial B$ were additionally smoothed for each fixed temperature and then were fitted with the help of Eq. (S3). It is found that the shape of the best fit curved is practically independent of the J choice from the set $J=1/2$, $J=3/2$, and $J=5/2$ (Fig. 2S, a). The obtained parameters $M_{s\rm LMM}(T)$ and $B_{0\rm LMM}(T)$ were used for plotting of the LMM magnetization field dependences (Fig. 2S, b). It is visible that in the resonance field $B_{\rm res}$ corresponding to the data of [11] the saturation of the $M_{\rm LMM}(B,T)$ field dependences is almost reached (Fig. 2S, b).

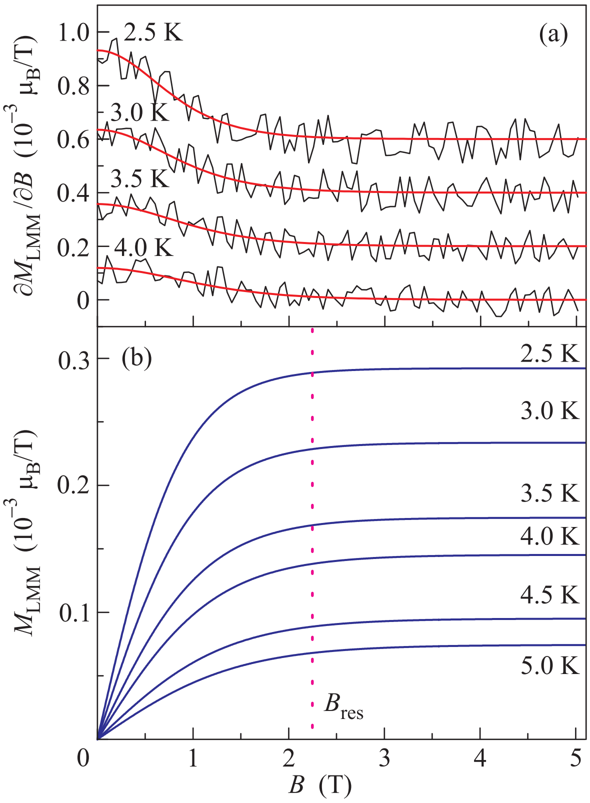

Fig. 2S. Curves $\partial M_{\rm LMM}/\partial B$, describing contribution of the paramagnetic centers to SmB_6 magnetization at different temperatures (a) and corresponding field dependences of magnetization $M_{\rm LMM}(B)$ (b). In the panel (a) smooth curves are the best fits to experimental data, which were used for calculation of the $M_{\rm LMM}(B)$ dependences in the panel (b). Experimental data and their approximations in the panel (a) are artificially shifted by fixed step $0.2\cdot10^{-3}\mu_{\rm B}/T$ for clarity. Dashed line denotes the field $B_{\rm res}$, where magnetic resonance in SmB_6 was observed (see reference [11] of the main text)

We wish to mark that for any J the $B_{0\rm LMM}$ temperature dependence followed linear law $B_{0\rm LMM}(T)\sim\theta(T)=T-T_0$ within fitting errors. Temperature dependences $B_{0\rm LMM}(T)$ were used for calculation of the effective magnetic moments μ^* for the different choices of J and extrapolation type for $M_{s\rm Pauli}(T)$. The result was weakly sensitive to extrapolation function used and was mainly controlled by the quantum number J. It follows from the Table 1 that big $\mu^*\sim(7\text{–}14)\mu_B$ may be expected for SmB_6.

Now let us consider an estimate of the localized magnetic moments concentration $N(T)$. To get a higher estimate, one needs to consider linear extrapolation of $M_{s\rm Pauli}(T)$ because in this case the contribution to magnetization from LMM is enhanced (Fig. 2b of the main text). As long as in SmB_6 the dependence $B_{0\rm LMM}(T)$ is temperature linear the condition $\mu^*(T)=\text{const}$ holds and, consequently, the observed temperature dependence $M_s(T)=N(T)\mu^*$ is caused by increase of LMM concentration with lowering temperature. The

Table 1. Effective magnetic moment, LMM saturated magnetization per Sm ion and concentration of the localized magnetic moments in SmB_6

J	μ^*/μ_B	$M_{s\mathrm{LMM}}/\mu_B$, $T = 2.5\,\mathrm{K}$	N/N_{Sm}, $T = 2.5\,\mathrm{K}$
1/2	6.6 ± 0.1	$(0.30 \pm 0.05) \cdot 10^{-3}$	$4.5 \cdot 10^{-5}(2 \cdot 10^{-3})$
3/2	11.8 ± 0.2	$(0.31 \pm 0.06) \cdot 10^{-3}$	$2.6 \cdot 10^{-5}(4 \cdot 10^{-4})$
5/2	13.9 ± 0.3	$(0.31 \pm 0.06) \cdot 10^{-3}$	$2.2 \cdot 10^{-5}(2 \cdot 10^{-4})$

data M_s and μ^* suggest that this concentration is low and, even for $T = 2.5\,\mathrm{K}$, does not exceed $(2.2-4.5) \cdot 10^{-5}$ of samarium ions concentration (see last column of the Table 1). This value is, apparently, much less than the concentration of Sm^{3+} ions $N_{\mathrm{Sm}(3+)}$, which number is about half of the total number of samarium ions (see [6] of the main text). If localized magnetic moments in SmB_6 are identified with spin-polaron states, it is necessary to take into account the renormalization of $M_{s\mathrm{LMM}}$ ([19] of the main text). This will result in enhancement of expected LMM concentration by the factor 9–40 (see figures in brackets in the last column of the Table 1). However, even in the latter case $N(T) \ll N_{\mathrm{Sm}(3+)}$.